Russ. J. Numer. Anal. Math. Modelling, Vol. 20, No. 6, pp. 549–562 (2005)

On new possibilities of increasing transmission capacity of high-speed fiber-optic communication lines

Yu. I. SHOKIN,* E. G. SHAPIRO,† M. P. FEDORUK,* and S. K. TURITSYN†

Abstract — In this paper we propose several ways of increasing the information capacity of data transmission based on the combination of the technologies of dispersion control, distributed amplification, spectral channel multiplexing, and optical regeneration of signals. The results of mathematical modelling can be used for upgrading existing lines and designing the next generation of trunk high-speed fiber-optic communication lines.

1. INTRODUCTION

In view of considerable progress in the development of fiber-optic communication, systems with the total information transmission rate greater than 1 Tbit/s will find a wide commercial application within the next few years. However, since the number of Internet users is permanently growing, even these rates will not be able to satisfy their permanently increasing demand.

At the present stage, soliton communication lines with dispersion control are regarded as the most probable candidates for the development of trunk superfast lines (with transmission rate 40 Gbit/s and more per frequency channel). Dispersion control systems use periodically alternating optical fibers with chromatic dispersion of opposite signs, which allows one to control the dispersive pulse broadening, increase the power-to-noise ratio of a signal, and decrease optical pulse degeneration caused by nonlinear effects (see, e.g. [1]).

Mathematical modelling is of fundamental importance for the study of fiber-optic communication lines, because the analytical methods for studying these systems are rather limited and laboratory experiments call for great expenses and are often impossible.

The propagation of optical pulses along a fiber-optic transmission line is described by the generalized nonlinear Schrodinger equation for the complex envelope

*Institute of Computational Technologies, Siberian Branch of the Russian Academy of Sciences, Novosibirsk 630090, Russia

†Institute of Automatics and Electrometry, Siberian Branch of the Russian Academy of Sciences, Novosibirsk 630090, Russia

The work was supported by the Federal Program of Leading Scientific Schools (SS-2314.2003.1) and the Siberian Branch of the Russian Academy of Sciences (Project No. 2003-2).

A of the electromagnetic field [3]

$$\mathrm{i}\frac{\partial A}{\partial z}+\mathrm{i}(\gamma-g)A-\frac{\beta_2}{2}\frac{\partial^2 A}{\partial t^2}-\frac{\beta_3}{6}\frac{\partial^3 A}{\partial t^3}+\sigma\left[|A|^2A+\frac{\mathrm{i}}{\omega}\frac{\partial}{\partial t}\left(|A|^2A\right)-T_RA\frac{\partial|A|^2}{\partial t}\right]=0. \tag{1.1}$$

Here z is the distance along the line, t is the time, $|A|^2$ is the power, β_2 is the dispersion parameter of the group rate, β_3 is the third-order dispersion, T_R is the time of the Raman response, σ is the Kerr nonlinearity factor, γ is the attenuation factor, g is the signal amplification factor. The values β_2, β_3, σ, γ, and g are given as functions of z to take into account the variations of these parameters in passing from one type of optical fiber to another.

The nonlinearity factor σ is specified by the formula $\sigma=(2\pi n_2)/(\lambda A_{\mathrm{eff}})$, where n_2 is the nonlinear refractive index, λ is the wavelength carrier, $\omega=c_l/\lambda$ is the radial frequency of the carrier signal, c_l is the speed of light, A_{eff} is the effective area of the eigenmode of the optical fiber.

To solve numerically equation (1.1) we used the method of splitting over physical processes. Let us write this equation in the operator form:

$$\frac{\partial A}{\partial z}=\left(\tilde{D}+\tilde{N}\right)A$$

where $\tilde{D}$ is the operator of the linear part that takes into account the dispersion effects and attenuation (amplification), and $\tilde{N}$ is a nonlinear operator

$$\begin{aligned}\tilde{D}&=-\gamma+g-\mathrm{i}\frac{\beta_2}{2}\frac{\partial^2}{\partial t^2}+\frac{\beta_3}{6}\frac{\partial^3}{\partial t^3}\\ \tilde{N}&=\mathrm{i}\sigma\left[|A|^2+\frac{\mathrm{i}}{\omega_0}\frac{1}{A}\frac{\partial}{\partial t}\left(|A|^2A\right)-T_R\frac{\partial|A|^2}{\partial t}\right].\end{aligned}$$

The solution of the nonlinear Schrodinger equation can be formally written as

$$A(z+h,t)=\exp\left[\int_z^{z+h/2}\tilde{N}(s)\mathrm{d}s\right]\exp[h\tilde{D}]\exp\left[\int_{z+h/2}^{z+h}\tilde{N}(s)\mathrm{d}s\right]A(z,t). \tag{1.2}$$

The operator $\exp\left[h\tilde{D}\right]$ is calculated in the Fourier space

$$\exp\left[h\tilde{D}\right]A\left(z,t\right)=\left\{F^{-1}\exp\left[h\tilde{D}\left(i\omega\right)\right]F\right\}A\left(z,t\right).$$

We can show that the scheme is of the second-order of accuracy with respect to the step h (see [3]).

The value of a bit-error rate that determines the number of erroneous bits per total number of transmitted bits is the estimate of the communication system quality [2]. The acceptable value of the bit-error rate is $\mathrm{BER}\leqslant 10^{-9}$, which corresponds to one erroneously recorded bit per 10^9 transmitted bits. We define the values P_1 and P_0

as the probabilities of error in recording ‘1’ and ‘0’, respectively. In turn, the given values are defined as [2]

$$P_1 = \int_{-\infty}^{I_d} p_1(x)\mathrm{d}x, \quad P_0 = \int_{I_d}^{\infty} p_0(x)\mathrm{d}x.$$

Suppose that the probability densities of zero and unity p_i, $i = 0, 1$, are distributed by the normal law

$$p_i(x) = \frac{1}{\sqrt{2\pi}\sigma_i} \exp\left[-\frac{(x-\mu_i)^2}{2\sigma_i^2}\right]$$

where μ_i are the mean values, σ_i is dispersion, I_d is the solvability level defined from the minimality condition of the bit-error rate BER $= (P_1 + P_0)/2$. We further introduce the value of the Q-factor which is connected with BER:

$$\mathrm{BER} = \frac{1}{2}\mathrm{erfc}\left(\frac{Q}{\sqrt{2}}\right) \approx \frac{\exp(-Q^2/4)}{\sqrt{2\pi}Q} \tag{1.3}$$

where

$$Q = \frac{\mu_1 - \mu_0}{\sigma_1 + \sigma_0}.$$

Note that the bit-error rate BER $\leqslant 10^{-9}$ is associated with $Q \geqslant 6$. We use in this work the standard value of the Q-factor as the quality criterion of signal transmission. The data transmission distance is defined as the distance for which the value of the Q-factor is $Q \geqslant 6$. In order to calculate the data transmission distance, we used in the calculations more than five pseudorandom sequences of 128 bits each and the transmission range in each of the channels was defined as the median average of the distances calculated in each sequence [10]. Next, the transmission length was taken as the shortest distance in all possible channels.

There are two most probable ways for further increasing the information capacity of fiber-optic communication systems [4]: increasing the total number of frequency channels in spectral multiplexing systems and increasing the information transmission rate in an individual channel.

In this paper we propose several ways for increasing the information capacity of data transmission on the basis of the combination of the technologies of dispersion control, distributed amplification, spectral channel multiplexing, and optical signal regeneration.

2. USE OF RAMAN AMPLIFIERS FOR INCREASING TRANSMISSION CAPACITY OF FIBER-OPTIC COMMUNICATION LINES

The principle of operation of distributed Raman amplifiers (DRAs) [5] is based on induced Raman scattering. Since distributed amplification provides a low level of noise, the distance between the amplifiers can be increased. This circumstance is important for domestic fiber communication lines. In the simplest Raman amplification model used in the work, the depletion of a pump wave is neglected and its exponential decay along the optical fiber length is assumed. In this case, for example for reverse Raman pumping along the length L the amplification factor has the form

$$g(z) = g_0 \exp[-2\gamma_p(L-z)].$$

Here the value g_0 is proportional to the pump power and γ_p is the attenuation coefficient of the signal amplitude at the pump wavelength.

Any type of optical amplifier, besides amplifying the input optical signal, adds to it the noises of amplified spontaneous emission (ASE). The presence of ASE deteriorates the signal-to-noise ratio of the system, increases the bit-error rate, and deteriorates the transmission characteristics of the fiber transmission line. The model of ‘white’ noise that is added to the system in each amplifier is used as the initial mathematical model for describing spontaneous emission noises.

In the case of Raman fiber amplifiers, the ‘white’ noise spectral density was calculated by the formula

$$S_{sp} = 2g(z)\delta z n_{sp} h\nu$$

where h is the Plank constant, ν is the signal frequency, δz is the typical value of the variation of the function $g(z)$, and the value of the spontaneous emission factor n_{sp} was defined as

$$n_{sp} = 1 + \frac{1}{\mathrm{e}^{(h\nu)/(kT)} - 1}.$$

We show the basic possibility to increase the total rate of information transmission in Raman amplifiers from 2.5 Gbit/s to 160 Gbit/s using the numerical modelling of the Novosibirsk–Omsk channel as an example [9].

The Novosibirsk–Omsk line consists of four sections of standard one-mode fiber (SMF) of length 127 km, 135 km, 138 km, and 163 km [9]. At the end of each piece of optical fiber there is an electric regenerator that restores the optical pulse form. However, the use of these regenerators limits the data transmission rate to 2.5 Gbit/s.

In order to increase the line transmission capacity we propose to use the technologies of dispersion control and spectral multiplexing of channels. We replace the electric regenerators at the end of each SMF segment by commercial modules with optical dispersion compensation fiber (DCF). The lengths of DCF pieces are chosen so that the average line dispersion $\langle D\rangle$ is close to zero. To compensate for the optical losses in each SMF+DCF section we use the fiber Raman amplifier.

We carried out calculations for a spectral multiplexing four-channel system with separation 0.8 nm (100 GHz) at wavelength 1548.8 nm, 1548.88 nm, 1548.96 nm, and 1549.04 nm. The data transmission rate in each channel amounted to 40 Gbit/s.

Below we give the graphs of the Q-factor, which is calculated after the transmission through the worst (as to the value of the Q-factor) of the four channels, versus the optical pulse width with fixed average power 0.5 dBm (Fig. 1) and versus the

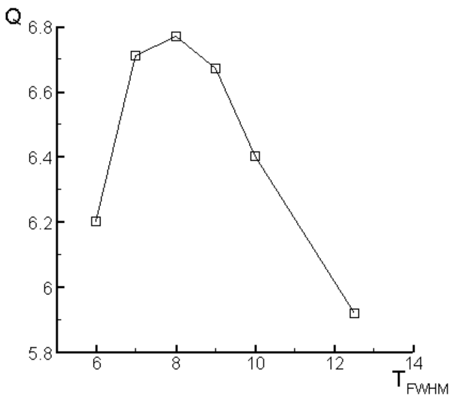

Figure 1. Q-factor versus optical pulse width T_{FWHM} (ps).

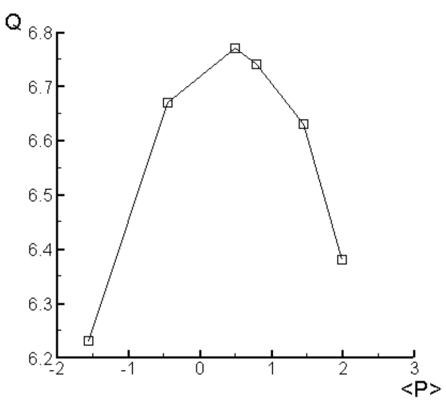

Figure 2. Q-factor versus average pulse power $\langle P \rangle$ (dBm).

average power with fixed pulse width 8 ps (Fig. 2). Figures 1 and 2 clearly demonstrate the existence of modes resistant to width and power variation at which the Q-factor is larger than 6.

3. USE OF FLAT-TOP FORMAT FOR INCREASING DATA TRANSMISSION SPECTRAL EFFICIENCY

A further increase in the transmission capacity of fiber-optic communication lines is possible by increasing the spectral efficiency of data transmission. In the past decade great interest has been shown in high-rate (40 Gbit/s and more) technologies of data transmission with densely located frequency channels.

We investigate data transmission in $N \times 40$ Gbit/s spectral multiplexing systems using a flat top format along the frequency band B and the signal time profile $\sin(\pi Bt)/t$. Using pulses of this shape, the strong interaction of neighbouring bits

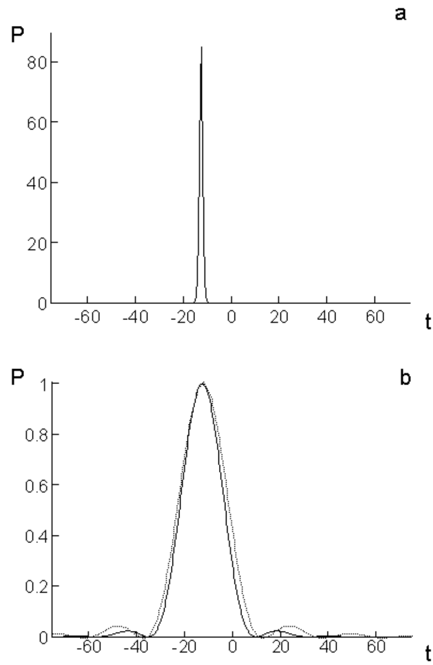

Figure 3. Time profile of pulse power P (mW) before (Fig. 3a) and after supergaussian optical filter (Fig. 3b).

can be suppressed by the resonance arrangement of zeros in the function $\sin(\pi Bt)/t$ at the centers of bit intervals.

In order to produce sinc-shaped signal carriers with a limited spectrum, a short gaussian pulse (1.7 ps) was first put through a supergaussian optical filter. Figure 3 shows the time profile of the pulse in front of and behind the optical filter, respectively. The dotted curve in Fig. 3 corresponds to the plot of the function $\sin(\pi Bt)/t$. Note that the optical filter width B is chosen so that zeros in the function $\sin(\pi Bt)/t$ are at the centers of bit intervals. In view of this, the interaction between the neighbouring bits decreases.

With no loss of generality, we consider the propagation of sinc-shaped signals in the spectral multiplexing communication system whose periodic section has the following configuration:

$$\mathrm{SMF}(20\ \mathrm{km}) + \mathrm{DCF}(6.8\ \mathrm{km}) + \mathrm{SMF}(20\ \mathrm{km}) + \ \mathrm{EDFA}.$$

Here EDFA (erbium-doped fiber amplifier) is an erbium fiber-optic amplifier.

In the case of erbium-doped fiber amplifiers, the spectral 'white' noise density is calculated by the formula [2]

$$S_{sp} = (G-1)n_{sp}h\nu.$$

The spontaneous emission factor n_{sp} is related to the amplifier noise figure NF by

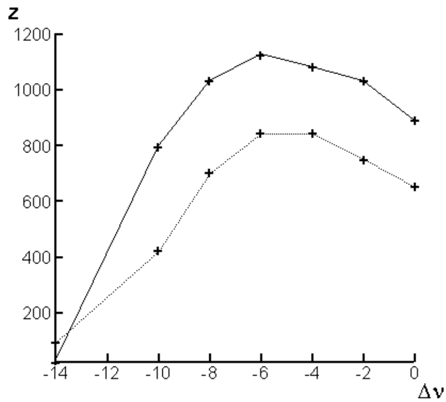

Figure 4. Signal propagation distance z (km) versus the value of optical filters shear $\Delta\nu$ (GHz).

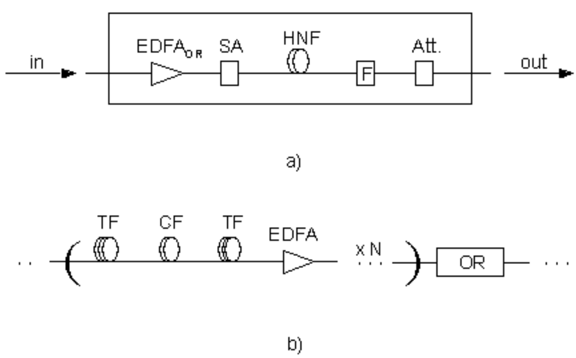

Figure 5. Schematic optical regenerator diagram (Fig. 5a) and symmetric fiber-optic communication line (Fig. 5b).

the relation

$$\mathrm{NF} = 2n_{sp}(G-1)/G.$$

Here G is the gain coefficient of the erbium-doped fiber amplifier. Note that erbium fiber-optic amplifiers are called lumped amplifiers, because the length on which the signal is amplified (several tens of meters) is much less than the distance between the amplifiers (several tens of kilometers). In this case, the signal gain in equation (1.1) has the form

$$g(z) = \sqrt{G}\delta(z-z_k)$$

where z_k are amplifier locations.

Let us consider data transmission in eight frequency channels in the wavelength range of 1548.78 – 1551.98 nm. The distance between the neighbouring channels is 0.4 nm (50 GHz). The mixing and separation of channels are done by a super-gaussian sixth-order filter of width 43 GHz and a preset optimal shift relative to the

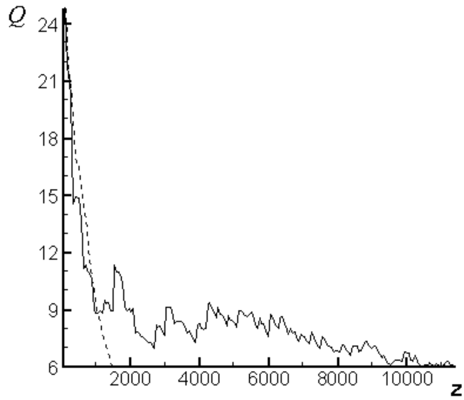

Figure 6. Q-factor versus propagation distance z (km) in one of frequency channels in the system with an optical regenerator (solid line) and without it (dotted line) for the symmetric dispersion pattern TF + CF + TF.

channel center. It should be emphasized that the value of the optical filter shift $\Delta\nu$ relative to the frequency channel center is a very important parameter of the problem. Figure 4 shows the propagation distance as the function of the optical filter shift relative to the channel center for a supergaussian sixth-order filter (solid line) and a rectangular filter (dotted line). Note that the optimal shift depends on the shape of the optical filter. For example, the optimal shift for the supergaussian sixth-order filter is 6 GHz.

Thus, direct numerical modelling shows that data transmission with spectral efficiency 0.8 bit/s/Hz in $N \times 40$ Gbit/s spectral multiplexing systems at distances of more than 1100 km without data correction is possible [8].

4. USE OF OPTICAL 2R REGENERATORS FOR INCREASING INFORMATION CAPACITY OF FIBER-OPTIC COMMUNICATION LINES

One of the promising ways to considerably increase the information capacity of trunk fiber-optic communication lines is to use optical signal regenerators. Let us consider the results of modelling a fiber-optic communication line with spectral multiplexing of channels with built-in 2R optical regenerators on the basis of a saturable absorber (SA). The principle of operation of the given unit is based on the absorption of the input optical signal power if it turns out to be lower than some threshold power P_{sat}. With power higher than P_{sat}, the SA transmittance rapidly increases and asymptotically approaches unity. Under these conditions, the low-power radiation of the amplified spontaneous noise and the background dispersive radiation are suppressed by the SA. The use of the SA in combination with a narrow band optical filter and a highly nonlinear fiber (HNF) allows one to suppress noises in unit bits. The structure of the optical regenerator (OR) is shown in Fig. 5a.

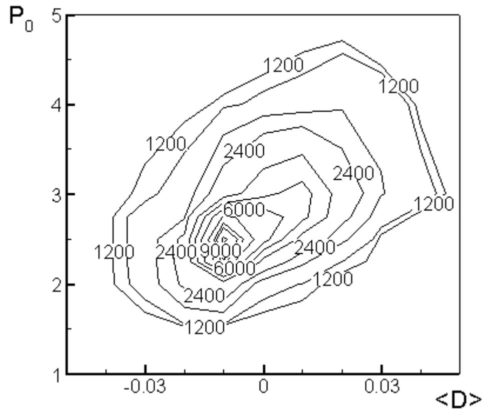

Figure 7. Isolines of data transmission distance in the plane (average dispersion, peak power) for the line PSCF + RDF + PSCF + EDFA.

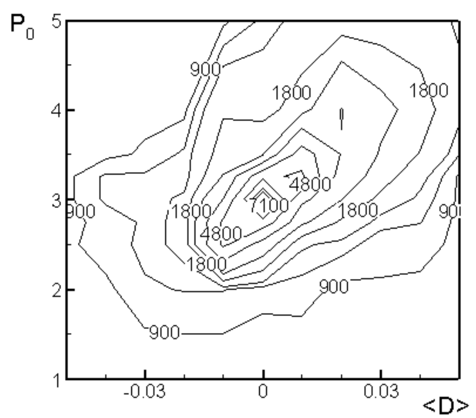

Figure 8. Isolines of data transmission distance in the plane (average dispersion, peak power) for the line TL + RTL + TL + EDFA.

The input signal triggered in the optical regenerator is first amplified by the erbium-doped fiber amplifier ($EDFA_{OR}$). Then the pulse is saturated in the SA. The loss function $\alpha(t)$ in the SA, which is dependent on the time and power of the input signal, is described by the ordinary differential first-order equation:

$$\frac{d\alpha(t)}{dt} = -\frac{\alpha(t) - \alpha_0}{\tau} - \frac{\alpha(t) P(z^*, t)}{\tau P_{sat}} \tag{4.1}$$

where $P(z^*, t) = |A(z^*, t)|^2$ is the power distribution of the input signal, $\alpha_0 = -3$ dB is the constant loss, $z^* \equiv \text{const}$ is the fixed distance, P_{sat} is the threshold saturation power, and τ corresponds to the pulse decay time. To find the function $\alpha(t)$, we solve a boundary value problem with periodic boundary conditions $\alpha(0) = \alpha(T)$, where T is the duration of the bit sequence. Then the transfer function $S(t) = 1 -$

$\alpha(t, P(z^*, t))$, and the effect of the saturable absorber on the signal is described by

$$P_{\text{out}}[z^*, t) = [1 - \alpha(t, P_{\text{in}}(z^*, t))]P_{\text{in}}(z^*, t) = S(t)\, P_{\text{in}}(z^*, t)\,. \tag{4.2}$$

Then the signal propagates in the HNF with anomalous dispersion. Since the pulse has a considerable energy, it becomes narrower when passing through the HNF due to phase self-modulation and its spectrum, accordingly, becomes broader. Next, an optical filter (F) is set up, it provides losses which are greater if the input pulse energy is higher. Thus, the signal energy is self-regulated. The width of the optical filter that has the gaussian form amounts to 100 –120 GHz. The optimal HNF length is 3–6 km. At the output from the OR the average signal power is restored to its initial value by a unit called an attenuator.

We consider examples of the optimization of the 4×40 Gbit/s symmetric fiber-optic communication line (see Fig. 5b) with periodic cell length 60 km and the distance between the optic regenerators 300 km [11]. The periodic section of this line consists of two equal pieces of transmission fiber (TF) with positive dispersion and between them there is a piece of dispersion-compensating fiber (CF) with negative dispersion. The types of optical fibers and their parameters used in the calculations are given in Table 1.

The distance between the neighbouring frequency channels was 1.6 nm (200 GHz). An individual optical regenerator was employed for each channel after the signal demultiplexing.

We give some computational results for two configurations of symmetric fiber-optic communication lines:

$$\text{PSCF} + \text{RDF} + \text{PSCF} + \text{EDFA}$$

$$\text{TL} + \text{RTL} + \text{TL} + \text{EDFA}.$$

To calculate the transmission length we used from 5 to 11 pseudorandom sequences of 128 bits each.

The typical behaviour of the Q-factor versus the distance is shown in Fig. 6. As seen, the presence of optical regenerators in the system allows one to considerably increase the distance for which $Q \geqslant 6$.

The results of extensive numerical calculations are presented in Figs. 7 and 8. Figure 7 shows the results of the optimization of the line PSCF + RDF + PSCF + EDFA. The calculations showed that it is possible to attain the data transmission range over 10,000 km by the proper choice of the optical regenerator parameters, input peak pulse power, and the average line dispersion. The corresponding system without optical regenerators demonstrates the propagation range about 2000 km.

Figure 8 shows the results of the optimization of the line TL + RTL + TL + EDF. Here, with optimal parameters of the system, the propagation range over 8000 km becomes possible.

Table 1.
Types of optical fibers and their parameters.

PSCF	Attenuation at wavelength 1550 nm	0.18 dB/km
	Effective mode area	110 μm^2
	Dispersion	20 ps/nm/km
	Dispersion slope	0.06 ps/nm^2/km
	Nonlinear refraction index	2.7×10^{-20} m^2/W
RDF	Attenuation at wavelength 1550 nm	0.3 dB/km
	Effective mode area	20 μm^2
	Dispersion	−42 ps/nm/km
	Dispersion slope	−0.13 ps/nm^2/km
	Nonlinear refraction index	2.7×10^{-20} m^2/W
TL	Attenuation at wavelength 1550 nm	0.21 dB/km
	Effective mode area	60 μm^2
	Dispersion	8 ps/nm/km
	Dispersion slope	0.08 ps/nm^2/km
	Nonlinear refraction index	2.7×10^{-20} m^2/W
RTL	Attenuation at wavelength 1550 nm	0.28 dB/km
	Effective mode area	28 μm^2
	Dispersion	−16 ps/nm/km
	Dispersion slope	−0.16 ps/nm^2/km
	Nonlinear refraction index	2.7×10^{-20} m^2/W
HNF	Attenuation at wavelength 1550 nm	0.5 dB/km
	Effective mode area	6.5 μm^2
	Dispersion	2 ps/nm/km
	Dispersion slope	0.03 ps/nm^2/km
	Nonlinear refraction index	2.7×10^{-20} m^2/W

5. USE OF NONLINEAR INFORMATION TRANSMISSION MODES IN OPTICAL COMMUNICATION LINES

A decrease in the total chromatic dispersion allows one to suppress the fluctuation of separate bits positions – the so-called Gordon–Haus effect [7]. Therefore, when designing fiber-optic communication lines, zero average dispersion is often fixed. In this section, however, it is shown that in some situations a rather large absolute value of average chromatic dispersion $\langle D \rangle$ provides better quality of signal transmission than linear modes in which the absolute value of the average dispersion is close to zero. These modes are essentially nonlinear, though the average dispersion symbol does not correspond to the classical soliton cases of signal propagation.

We considered an optical system consisting of 17 sections of the form

$$\text{SMF(85 km) + EDFA + DCF(15 km) + EDFA.}$$

Here SMF is the standard one-mode fiber, DCF is the dispersion-compensating fiber. Each section has two amplifiers with amplification factors that allow one to fully compensate for the signal attenuation in the corresponding fibers. The total losses of one section amounted to 26.8 dB. The residual dispersion of the line was

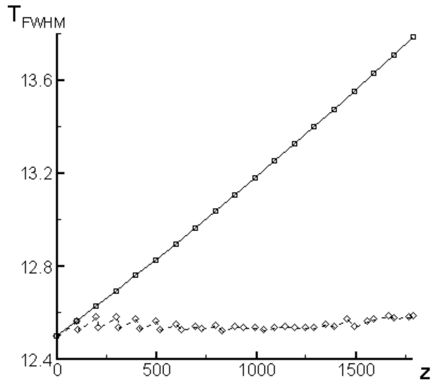

Figure 9. Optical pulse width T_{FWHM} (ps) versus propagation distance. Solid curve – $\langle D\rangle = 0$, dash-dot curve – $\langle D\rangle = -0.65$ ps/nm/km.

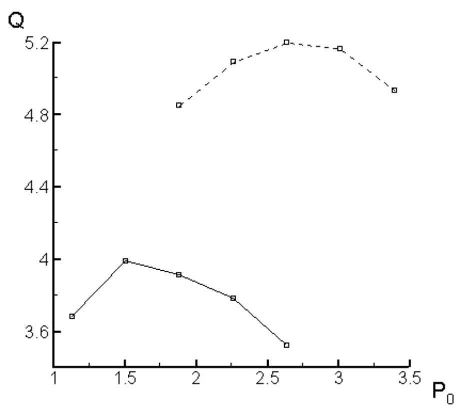

Figure 10. Q-factor versus input peak signal power P_0 (mW). Solid line – $\langle D\rangle = 0$, dash-dot line – $\langle D\rangle = -0.65$ ps/nm/km.

compensated by an additional segment of the standard one-mode fiber (SMF). The parameters of optical fibers are presented in Table 2.

Figure 9 shows the dependences of the optical pulse width on the distance z at the points of its minimal width (the so-called chirpless points) for the gaussian input signal of initial width 12.5 ps, which are obtained from the numerical solution of equation (1.1) with the average dispersion values $\langle D\rangle = 0$ and $\langle D\rangle = -0.65$ ps/nm/km, respectively.

As seen, with small negative values of average dispersion and with zero average dispersion, the optical pulse broadens. An increase in the absolute value of the negative average dispersion stabilize the signal width. Thus, the regimes with relatively large negative average dispersion $\langle D\rangle = -0.65$ ps/nm/km or $\langle D\rangle = -0.8$ ps/nm/km admit a quasistable nonlinear propagation regime without significant 'spreading' of optical pulses, which decreases the role of the interaction between the neighbouring

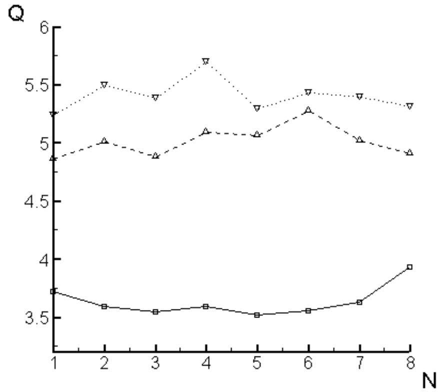

Figure 11. Q-factor versus the channel number N for $\langle D \rangle = 0, -0.35, -0.8$ ps/nm/km (from bottom upwards).

Table 2.
Types of optical fibers and their parameters.

SMF	Fiber loss at wavelength 1550 nm	0.2dB/km
	Effective mode area	80 μm^2
	Dispersion	17 ps/nm/km
	Dispersion slope	0.07 ps/nm^2/km
	Nonlinear refraction index	2.7×10^{-20} m^2/W
DCF	Fiber loss at wavelength 1550 nm	0.65 dB/km
	Effective mode area	19 μm^2
	Dispersion	-100 ps/nm/km
	Dispersion slope	-0.41 ps/nm^2/km
	Nonlinear refraction index	2.7×10^{-20} m^2/W

bits. This allows one for a chosen pulse width to use stronger input signals, which, in turn, improves the signal-to-noise ratio without significant deterioration of the signal quality because of nonlinearity.

The numerical modelling of optical pulse propagation in eight channels at wavelengths 1550.1–1555.8 nm with separation 0.8 nm (100 GHz) between the neighbouring channels and the transmission rate of 40 Gbit/s in a single frequency channel was implemented. To calculate the value of the Q-factor at the end of the line, we used in the calculation 25 pseudorandom sequences of 128 bits each. Figure 10 shows the Q-factor in the worst channel versus the peak power of the input pulse with average dispersions $\langle D \rangle = 0$ and $\langle D \rangle = -0.65$ ps/nm/km. The optimal value of the peak power of the input signal with $\langle D \rangle = -0.65$ ps/nm/km is larger than that for zero dispersion. However, a decrease in the negative role of the nonlinear effects in this case leads to a decrease in the error bit rate (an increase in the Q-factor). Figure 11 shows the values of the Q-factor in eight channels at the end of the line with $z = 1700$ km for the following values of the average system dispersion (from the bottom upwards, respectively): $\langle D \rangle = 0, -0.35, -0.8$ ps/nm/km.

Thus, the results of numerical modelling show that the nonlinear regimes of data transfer along the communication line with negative average dispersion of order -1 ps/nm/km consisting of pieces of the standard one-mode fiber (SMF) and the dispersion-compensating fiber (DCF) demonstrate better quality of information transmission than the lines in which the absolute value of the average dispersion is close to zero (linear propagation). The value $Q \geqslant 4$ attained in nonlinear data transfer makes it possible to apply the method of forward error correction (FEC) to such lines [8].

REFERENCES

1. G. P. Agrawal, *Applications of Nonlinear Fiber Optics*. Academic Press, New York, 2001.
2. G. P. Agrawal, *Fiber-Optic Communication Systems*. John Wiley&sons, INC., New York, 1997.
3. G. P. Agrawal, *Nonlinear Fiber Optics*. Academic Press, New York, 2001.
4. E. M. Dianov, From terra-era to peta-era. *Vestnik Russ. Akad. Sci.* (2000) **70**, No. 11, 1010–1015 (in Russian).
5. E. M. Dianov, Raman fiber amplifiers. In: *Topical meeting on optical amplifiers and applications*. ThAI, Nara, June 9–11, 1999.
6. M. P. Fedoruk, A. G. Shapiro, and E.G. Shapiro, Modelling fiber-optic communication lines with Raman amplifiers. *Autometry* (2003) **39**, No. 4, 109–117 (in Russian).
7. J. P. Gordon and H. A. Haus, Random walk of coherently amplified solitons in optical fiber transmission. *Opt. Lett.* (1986) **11**, 665–668.
8. W. D. Grover, Forward error correction in dispersion-limited lightwave systems. *J. Lightwave Technol.* (1988) **6**, 643.
9. S. V. Shcheglyuk, S. K. Turitsyn, V. K. Mezentsev, and E. G. Shapiro, Methods for modelling transport optical networks. *Electrolink* (2002), No. 2, 43–46 (in Russian).
10. E. G. Shapiro, M. P. Fedoruk, and S. K. Turitsyn, Numerical estimate of BER in optical systems with strong patterning effects. *Electron. Lett.* (2001) **37**, No. 19, 1179–1181.
11. S. Waiyapot, S. K. Turitsyn, M. P. Fedoruk et al., Optical 2R regeneration at 40 Gbit/s using saturable in long-haul dispersion-managed fiber links. *Opt. Commmun.* (2004) **232**, 145–149.